Polyhedron 152 (2018) 94–101

Contents lists available at ScienceDirect

Polyhedron

journal homepage: www.elsevier.com/locate/poly

Synthesis, characterization and electrocatalytic H_2 production of phosphine-substituted CpFe complexes

Jin-Ping Li [a], Su-Ping Luo [b], Shu-Zhong Zhan [b], Yao-Cheng Shi [a,*]

[a] College of Chemistry and Chemical Engineering, Yangzhou University, Yangzhou 225002, China
[b] College of Chemistry and Chemical Engineering, South China University of Technology, Guangzhou 510640, China

ARTICLE INFO

Article history:
Received 13 March 2018
Accepted 5 June 2018
Available online 12 June 2018

Keywords:
CpFe complex
Iron carbonyl
Phosphine substitution
Cyclic voltammetry
H_2 production

ABSTRACT

Reaction of $Ph_2P(Se)CSNHPh$ with $Cp_2Fe_2(CO)_4$ in refluxing toluene affords complexes CpFe(CO)(k^{2}P,S-$Ph_2PC(S){=}NPh$) (**1**) and $CpFe(CO)_2$(kP-P(=Se)Ph_2) (**2**). Further, reactions of **2** with 1 equiv of PPh_2R in the presence of Me_3NO generate complexes CpFe(CO)(kSe-SeP(=Se)Ph_2)(L) (**3**, L = PPh_3; **4**, L = PPh_2Py). Unlike **2**, reactions of $CpFe(CO)_2$(kP-P(=S)Ph_2) with PPh_2R under the same conditions give the corresponding phosphine-substituted complexes CpFe(CO)(kP-P(=S)Ph_2)(L) (**5**, L = PPh_3; **6**, L = PPh_2Py). All the new compounds have been characterized by elemental analyses, IR, ^1H NMR, ^{13}C NMR and ^{31}P NMR spectroscopy and structurally determined by X-ray crystallography. Electrochemical studies indicate that using HOAc or TFA as a proton source complexes **1**–**6** can catalyze H_2 evolution.

1. Introduction

Nowadays the development of renewable energy is one of the most important challenges as global energy consumption is rising significantly. Molecular hydrogen is a carbon-free fuel that could become the energy carrier of the future, thus making the reversible interconversion of protons to molecular hydrogen a key process for future energy schemes. Nature is able to catalyze this process by a class of enzymes called hydrogenases. To date, three classes of hydrogenases, namely, the [FeFe]-, [FeNi]-, and [Fe]-hydrogenases, have been reported. The X-ray crystallographic structure determinations of the enzymes have revealed their active sites and allowed the mechanistic understanding of the catalytic process. Inspired by these insights, many FeFe and FeNi model complexes of the hydrogenase active sites have been synthesized [1–4]. However, because of the [Fe]-hydrogenase being a recent discovery, only a few small molecule mimics of [Fe]-hydrogenase have been reported [5–8]. In view of this reason, we have initiated a project for mimicking the [Fe]-hydrogenase [9]. As part of this ongoing work, herein we report syntheses and electrocatalytic H_2 production of CpFe complexes (Scheme 1).

2. Experimental

2.1. Materials and methods

All reactions were carried out under N_2 atmosphere with standard Schlenk techniques. All solvents employed were dried by refluxing over appropriate drying agents and stored under N_2 atmosphere. $Ph_2PCSNHPh$ [10], $Cp_2Fe_2(CO)_4$ [11] and $CpFe(CO)_2$(kP-P(=S)Ph_2) [12] were prepared according to literature methods. The progress of all reactions was monitored by TLC. ^1H NMR, ^{13}C NMR measurements were carried out on an Aglient 400 and ^{31}P NMR with the Bruker Avance 600 spectrometer. IR spectra were recorded on a BrukerTensor 27 spectrometer as KBr disks in the range 400–4000 cm^{-1}. Electrochemical measurements were made using a CHI660E potentiostat. Controlled potential coulometry experiments on 0.5 mM **1** (**2**) in 0.1 M $^nBu_4NPF_6/CH_3CN$ in the presence of 25 mM HOAc or TFA were conducted to confirm the catalytic production of hydrogen. Gas chromatography (GC) analysis of H_2 was conducted with an Agilent Technologies 7890A equipped with a thermal conductivity detector. Analyses for C, H and N were performed on an Elementar Vario EL analyzer. Melting points were measured on an X-4B apparatus and uncorrected.

2.2. Syntheses

2.2.1. Syntheses of **1**and **2**

To a stirred solution of $Ph_2PCSNHPh$ (6.428 g, 20 mmol) in CH_2Cl_2 (50 mL) was added elemental Se (1.896 g, 24 mmol). The

---

* Corresponding author.
E-mail address: ycshi@yzu.edu.cn (Y.-C. Shi).

https://doi.org/10.1016/j.poly.2018.06.009
0277-5387/

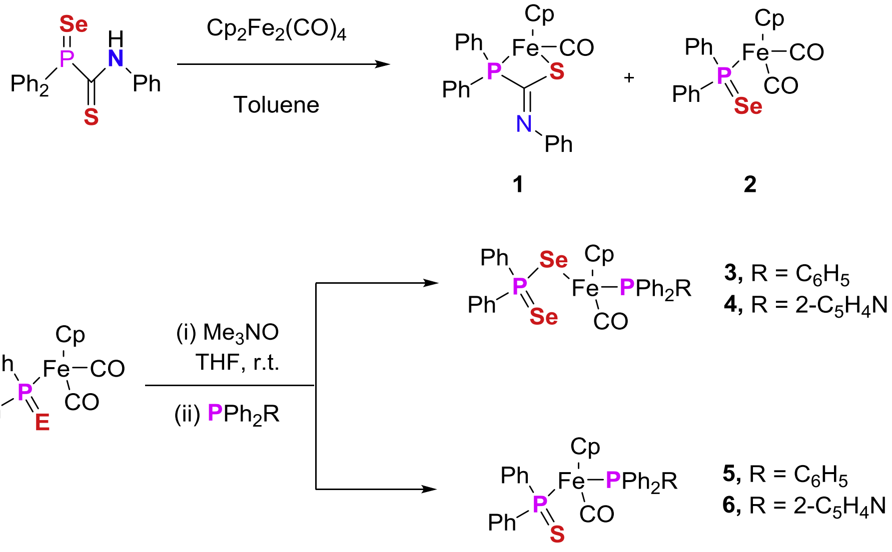

Scheme 1. Syntheses of complexes **1**–**6**.

reaction mixture was stirred for 3 h at room temperature, then the solvent was removed under reduced pressure, and the residue was recrystallized by acetonitrile to give a powdery solid that was dried under vacuum (6.165 g, yield 77%; mp, 98.7–100.4 °C). *Anal.* Calcd. for $C_{19}H_{16}NPSSe$ (%): C, 57.00; H, 4.03; N, 3.50. Found: C, 56.87; H, 4.12; N, 3.62. IR (KBr disk): 3150 (m), 3104 (w), 2997 (w), 2957 (w), 1593 (m), 1537 (s), 1485 (m), 1436 (m), 1384 (s), 1311 (w), 1180 (m), 1090 (m), 975 (w), 899 (w), 801 (w), 751 (s), 685 (s), 550 (s), 496 (m), 429 (w) cm^{-1}. ^1H NMR (400 MHz, $CDCl_3$, TMS): δ 12.01 (d, $J = 7.6$ Hz, 1H, NH), 8.10, 8.02–7.97, 7.55, 7.49–7.42, 7.31 (d, $J = 8.0$ Hz, 2H, m, 4H, t, $J = 7.6$ Hz, 2H, m, 6H, t, $J = 7.6$ Hz, 1H, $3C_6H_5$) ppm. ^{13}C NMR (100 MHz, $CDCl_3$, TMS): δ 186.72, 186.14 (C═S), 138.64, 138.51, 133.36, 133.26, 132.25, 132.22, 130.02, 129.21, 129.05, 128.42, 128.29, 127.59, 121.02 ($3C_6H_5$) ppm. ^{31}P NMR (243 MHz, $CDCl_3$, 85% H_3PO_4): δ 45.44 (s) ppm.

$Ph_2P(Se)CSNHPh$ (1.201 g, 3 mmol) and $Cp_2Fe_2(CO)_4$ (0.708 g, 2 mmol) were added to 15 mL of toluene. The solution was refluxed for 12 h, volatile components were removed in vacuo. The crude product was purified by TLC (silica gel, petroleum ether/ethyl acetate, v/v, 4:1), two orange-yellow bands in the decreasing order of R_f values offering **1** and **2** in respective yield of 23% (0.324 g) and 26% (0.344 g). For **1**, mp, 161.5–162.7 °C. *Anal.* Calcd. for $C_{25}H_{20}FeNOPS$ (%, **1**): C, 63.98; H, 4.30; N, 2.98. Found: C, 63.84; H, 4.21; N, 3.13. IR (KBr disk): 3070 (w), 1944 (vs), 1547 (s), 1478 (m), 1430 (m), 1308 (w), 1242 (w), 1194 (w), 1099 (m), 997 (w), 924 (m), 826 (m), 745 (m), 694 (s), 638 (w), 568 (m), 522 (m), 476 (w), 442 (w) cm^{-1}. ^1H NMR (400 MHz, $CDCl_3$, TMS): δ 8.00–7.96, 7.58–7.44, 7.37–7.31, 7.09 (m, 2H, m, 8H, m, 4H, t, $J = 6.8$ Hz, 1H, $3C_6H_5$), 4.50 (s, 5H, C_5H_5) ppm. ^{13}C NMR (100 MHz, $CDCl_3$, TMS): δ 218.97, 218.70 (CO), 148.12 (C═N), 136.24, 135.90, 134.00, 133.89, 131.29, 131.26, 130.79, 130.70, 130.21, 130.18, 128.94, 128.84, 128.61, 128.38, 128.28, 124.70, 122.25 ($3C_6H_5$), 81.09 (C_5H_5) ppm. ^{31}P NMR (243 MHz, $CDCl_3$, 85% H_3PO_4): δ 53.20 (s) ppm. For **2**, mp, 184.1–185.4 °C. *Anal.* Calcd. for $C_{19}H_{15}FeO_2PSe$ (%, **2**): C, 51.74; H, 3.43. Found: C, 51.59; H, 3.54. IR (KBr disk): 3054 (m), 2026 (vs), 1974 (vs), 1582 (w), 1475 (w), 1428 (m), 1359 (w), 1306 (w), 1272 (w), 1157 (w), 1118 (w), 1081 (m), 1000 (w), 929 (w), 847 (m), 749 (m), 693 (s), 621 (m), 574 (s), 508 (m), 421 (w) cm^{-1}. ^1H NMR (400 MHz, $CDCl_3$, TMS): δ 7.92–7.87, 7.37–7.33 (m, 4H, m, 6H, $2C_6H_5$), 4.93 (s, 5H, C_5H_5) ppm. ^{13}C NMR (100 MHz, $CDCl_3$, TMS): δ 212.41, 212.18 (2CO), 143.19, 142.75, 137.19, 137.08, 133.79, 133.60, 130.95, 130.84, 129.50, 129.48, 128.68, 128.50, 128.43, 127.96, 127.85 ($2C_6H_5$), 89.20 (C_5H_5) ppm. ^{31}P NMR (243 MHz, $CDCl_3$, 85% H_3PO_4): δ 75.89 (s) ppm.

2.2.2. Synthesis of **3**

The solution of 0.441 g (1 mmol) **2** and 0.262 g (1 mmol) PPh_3 in 30 mL of THF in the presence of 0.111 g (1 mmol) $Me_3NO{\cdot}2H_2O$ was stirred for 3 h at room temperature. After the solvent was removed under reduced pressure, the residue was subjected to TLC separation. Elution with petroleum ether/ethyl acetate (v/v, 4:1) afforded one orange-red band of **3** in yield of 18% (0.136 g). For **3**, mp, 164.8–165.6 °C. *Anal.* Calcd. for $C_{36}H_{30}FeOP_2Se_2$ (%, **3**): C, 57.32; H, 4.01. Found: C, 57.24; H, 4.17. IR (KBr disk): 3052 (w), 1933 (s), 1639 (s), 1464 (m), 1430 (m), 1377 (w), 1269 (w), 1180 (w), 1090 (m), 1023 (w), 993 (w), 890 (w), 826 (m), 745 (s), 691 (vs), 624 (w), 596 (m), 557 (s), 508 (s), 446 (w) cm^{-1}. ^1H NMR (400 MHz, $CDCl_3$, TMS): δ 8.32, 7.75–7.70, 7.60–7.55, 7.50–7.45, 7.34, 7.17, 6.88, 6.77 (t, $J = 9.6$ Hz, 2H, m, 5H, m, 2H, m, 8H, t, $J = 6.8$ Hz, 2H, t, $J = 6.8$ Hz, 2H, t, $J = 6.4$ Hz, 1H, t, $J = 7.2$ Hz, 2H, $5C_6H_5$), 4.44 (s, 5H, C_5H_5) ppm. ^{13}C NMR (100 MHz, $CDCl_3$, TMS): δ 220.91, 220.77, 220.61, 218.37 (CO), 147.57, 147.21, 141.08, 140.74, 134.72, 134.27, 133.85, 133.75, 132.69, 132.59, 132.10, 131.60, 131.57, 131.33, 130.96, 130.88, 130.86, 130.78, 129.91, 129.89, 128.59, 128.47, 128.01, 127.98, 127.82, 127.72, 127.26, 127.16, 127.05, 126.90, 126.87 ($5C_6H_5$), 89.14 (C_5H_5) ppm. ^{31}P NMR (243 MHz, $CDCl_3$, 85% H_3PO_4): δ 76.61 (s), 53.06 (s) ppm.

2.2.3. Synthesis of **4**

The solution of 0.441 g (1 mmol) **2** and 0.263 g (1 mmol) PPh_2Py in 30 mL of THF in the presence of 0.111 g (1 mmol) $Me_3NO{\cdot}2H_2O$ was stirred for 3 h at room temperature. After the solvent was removed in vacuo, the residue was subjected to TLC separation. Elution with petroleum ether/ethyl acetate (v/v, 4:1) afforded one orange-red band of **4** in yield of 17% (0.128 g). For **4**, mp, 166.3–167.7 °C. *Anal.* Calcd. for $C_{35}H_{29}FeNOP_2Se_2$ (%, **4**): C, 55.65; H, 3.87; N, 1.85. Found: C, 55.59; H, 3.77; N, 1.95. IR (KBr disk): 3052 (w), 1935 (s), 1571 (s), 1460 (s), 1378 (w), 1284 (vs), 1126 (m), 1074 (m), 1021 (w), 962 (w), 802 (w), 744 (m), 694 (s), 624 (w), 596 (w), 562 (m), 511 (m) cm^{-1}. ^1H NMR (400 MHz, $CDCl_3$, TMS): δ 8.38, 8.23, 7.73, 7.57, 7.37–7.30, 7.23–7.13, 6.89, 6.78 (d, $J = 4.0$ Hz, 1H, t, $J = 9.6$ Hz, 2H, t, $J = 8.4$ Hz, 2H, t, $J = 8.8$ Hz, 4H, m, 7H, m, 4H, s, 1H, t, $J = 6.8$ Hz, 1H, t, $J = 7.2$ Hz, 2H, $4C_6H_5$, $2\text{-}C_5H_4N$), 4.52 (s, 5H, C_5H_5) ppm. ^{13}C NMR (100 MHz, $CDCl_3$, TMS): δ 220.93, 220.64, 220.34 (CO), 158.36, 149.56, 147.80 (d, J = 69.0 Hz, d, J = 17.0 Hz, d, J = 37.0 Hz, C=N), 142.22, 141.89, 135.30, 134.86, 134.79, 134.73, 134.16, 134.07, 133.89, 133.80, 133.34, 132.92, 132.80, 131.13, 131.03, 130.95, 130.85, 130.12, 130.10, 129.93, 129.90, 128.82, 128.64, 128.17, 128.07, 127.95, 127.93, 127.82, 127.72, 127.29, 127.19, 127.08, 126.98, 126.95, 126.92, 123.44, 123.42 ($4C_6H_5$, 2-C_5H_4N), 88.92 (C_5H_5) ppm. ^{31}P NMR (243 MHz, $CDCl_3$, 85% H_3PO_4): δ 75.98 (s), 52.99 (s) ppm.

2.2.4. Synthesis of **5**

The solution of 0.394 g (1 mmol) $CpFe(CO)_2(kP\text{-}P(=S)Ph_2)$ and 0.262 g (1 mmol) PPh_3 in 30 mL of THF in the presence of 0.111 g (1 mmol) $Me_3NO{\cdot}2H_2O$ was stirred for 3 h at room temperature. After the solvent was removed under vacuum, the residue was subjected to TLC separation. Elution with petroleum ether/ethyl acetate (v/v, 4:1) afforded one orange-red band of **5** in yield of 24% (0.151 g). For **5**, mp, 173.4–174.7 °C. *Anal.* Calcd. for $C_{36}H_{30}FeOP_2S$ (%, **5**): C, 68.80; H, 4.81. Found: C, 68.63; H, 4.68. IR (KBr disk): 3051 (w), 1929 (vs), 1657 (w), 1578 (vs), 1466 (m), 1430 (w), 1374 (w), 1284 (s), 1127 (w), 1077 (m), 996 (w), 850 (w), 829 (w), 741 (m), 692 (s), 625 (w), 596 (m), 559 (m), 515 (m), 478 (w), 416 (w) cm^{-1}. ^{1}H NMR (400 MHz, $CDCl_3$, TMS): δ 8.00, 7.56–7.45, 7.33, 7.10 (s, 2H, m, 10H, s, 12H, t, J = 6.0 Hz, 1H, $5C_6H_5$), 4.50 (s, 5H, C_5H_5) ppm. ^{13}C NMR (100 MHz, $CDCl_3$, TMS): δ 219.00, 218.73 (CO), 137.17, 137.12, 137.10, 134.04, 133.93, 133.82, 133.65, 133.64, 131.35, 130.80, 130.71, 130.26, 128.99, 128.89, 128.71, 128.65, 128.49, 128.43, 128.33, 124.75, 122.28 ($5C_6H_5$), 81.14 (C_5H_5) ppm. ^{31}P NMR (243 MHz, $CDCl_3$, 85% H_3PO_4): δ 76.12 (s), 73.95 (s) ppm.

2.2.5. Synthesis of **6**

The solution of 0.394 g (1 mmol) $CpFe(CO)_2(kP\text{-}P(=S)Ph_2)$ and 0.263 g (1 mmol) PPh_2Py in 30 mL of THF in the presence of 0.111 g (1 mmol) $Me_3NO{\cdot}2H_2O$ was stirred for 3 h at room temperature. After the solvent was removed in vacuo, the residue was subjected to TLC separation. Elution with petroleum ether/ethyl acetate (v/v, 4:1) afforded one orange-red band of **6** in yield of 21% (0.132 g). For **6**, mp, 176.8–178.5 °C. *Anal.* Calcd. for $C_{35}H_{29}FeNOP_2S$ (%, **6**): C, 66.78; H, 4.64; N, 2.23. Found: C, 66.59; H, 4.71; N, 2.29. IR (KBr disk): 3054 (m), 1935 (s), 1573 (m), 1461 (vs), 1376 (m), 1282 (vs), 1185 (w), 1126 (m), 1075 (m), 1038 (w), 965 (w), 840 (m), 742 (vs), 697 (vs), 647 (w), 595 (w), 552 (w), 515 (s) cm^{-1}. ^{1}H NMR (400 MHz, $CDCl_3$, TMS): δ 8.72, 7.98, 7.55, 7.36, 7.18, 7.08 (s, 2H, s, 2H, s, 4H, s, 12H, s, 2H, s, 2H, $4C_6H_5$, 2-C_5H_4N), 4.50 (s, 5H, C_5H_5) ppm. ^{13}C NMR (100 MHz, $CDCl_3$, TMS): δ 219.01, 218.73 (CO), 150.28, 148.50 (d, J = 13.0 Hz, d, J = 22.0 Hz, C=N), 136.22, 135.87, 135.73, 134.28, 134.08, 134.01, 133.90, 131.33, 131.30, 131.11, 130.79, 130.69, 130.24, 130.21, 129.06, 128.97, 128.87, 128.64, 128.58, 128.40, 128.30, 124.72, 122.25, 122.21 ($4C_6H_5$, 2-C_5H_4N), 81.12 (C_5H_5) ppm. ^{31}P NMR (243 MHz, $CDCl_3$, 85% H_3PO_4): δ 76.14 (s), 74.30 (s) ppm.

2.3. X-ray structure determinations

Single crystals of $Ph_2P(Se)CSNHPh$ and **1**–**3**, **5** and **6** suitable for X-ray diffraction analyses were grown by slow evaporation of their CH_2Cl_2-petroleum ether solutions at 0–4 °C. For each compound, a selected single crystal was mounted on a Bruker D8quest CCD diffractometer using graphite-monochromated Mo-Kα radiation (λ = 0.71073 Å) at 295 K. Their structures were solved by direct methods using the SIR-2011 software and refined by full-matrix least-squares based on F^2 with anisotropic thermal parameters for all non-hydrogen using the SHELXTL program package [13]. All H atoms attached to C atoms were placed at geometrically idealized positions and subsequently treated as riding atoms, with C–H = 0.93 (Phenyl), 0.98 (Cyclopentadienyl) and U_{iso}(H) values of $1.2U_{eq}$(C). PLATON views of compounds are drawn using the PLATON software [14].

2.4. Electrochemistry of **1**–**6**

Cyclic voltammetry experiments were carried out in a ca 5-mL one-compartment glass cell. The working electrode was a glassy carbon disk (0.3 cm in diameter), the reference electrode an $Ag/AgNO_3$ (0.01 M $AgNO_3$/0.1 M $^nBu_4NPF_6$ in MeCN) electrode and the counter electrode a Pt wire. The electrolyte was 0.1 M $^nBu_4NPF_6$ in MeCN. The potentials (E) at the working electrode in all CV's are reported with respect to the Fc^+/Fc couple in electrolyte solution. The Fc^+/Fc coupling data were collected at the end of each experiment. All CV's reported are background-corrected, i.e. the scan with only electrolyte present was subtracted from the raw data. All background scans confirmed sufficient removal of O_2 as seen by the absence of a reduction peak at ca. −1.2 V. CV data were collected under flow of N_2 gas. The electrolyte solution was degassed by bubbling with N_2 for at least 10 min before measurement. The typical concentration of the organometallic complex was 1 mM. The acid concentration in the electrolyte was varied by addition of measured volumes of a solution of HOAc or TFA in MeCN.

3. Results and discussion

3.1. Syntheses

The reaction of $Ph_2P(Se)CSNHPh$, generated from the reaction of $Ph_2PCSNHPh$ and elemental selenium in dichloromethane, with $Cp_2Fe_2(CO)_4$ in refluxing toluene affords $CpFe(CO)(k^2P,S\text{-}Ph_2PC(S)=NPh)$ (**1**) and $CpFe(CO)_2(kP\text{-}P(=Se)Ph_2)$ (**2**). Further reactions of **2** with 1 equiv of PPh_2R in the presence of Me_3NO lead to complexes $CpFe(CO)(kSe\text{-}SeP(=Se)Ph_2)(L)$ (**3**, L = PPh_3; **4**, L = PPh_2Py). Some modified $FeCp(CO)_2$ complexes such as $CpFe(CO)_2X$ (X = $SeSO_2R$, $SeCO_2R$), $CpFe(CO)(k^2S,E\text{-}ECS_2Ph)$ [15], $CpFe(CO)(EPh_3)SeCOAr$ and $CpFe(CO)(PPh_3)SCO_2Ar$ [16] have been reported by El-khateeb. Unlike **2**, reactions of $CpFe(CO)_2(kP\text{-}P(=S)Ph_2)$ with PPh_2R under the same conditions lead to the corresponding phosphine-substituted complexes $CpFe(CO)(kP\text{-}P(=S)Ph_2)(L)$ (**5**, L = PPh_3; **6**, L = PPh_2Py). Also, it should be mentioned that several CpFe complexes such as $CpFe(CO)(PPh_3)TePh$, $CpFe(CO)(PPh_3)R$ [17] and $[CpFe(PR_3)(CO)(BNCAr_2)]^+[BAr_4^X]^-$ [18] have been synthesized by Pasynskii and Niemeyer.

3.2. X-ray structures

The molecular structures of $Ph_2P(Se)CSNHPh$ and **1**–**3**, **5** and **6** shown in Figs. 1–6 were determined by using X-ray diffraction

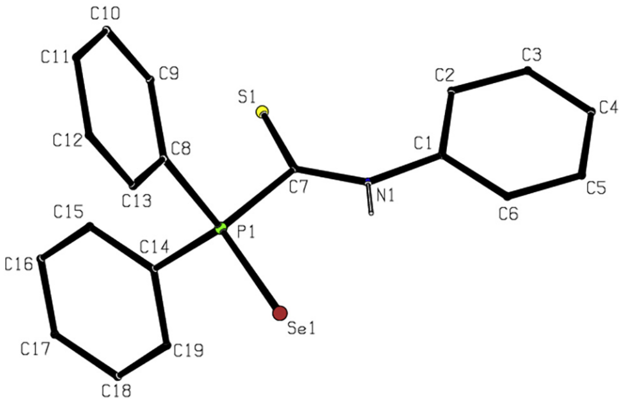

Fig. 1. PLATON view of $Ph_2P(Se)CSNHPh$.

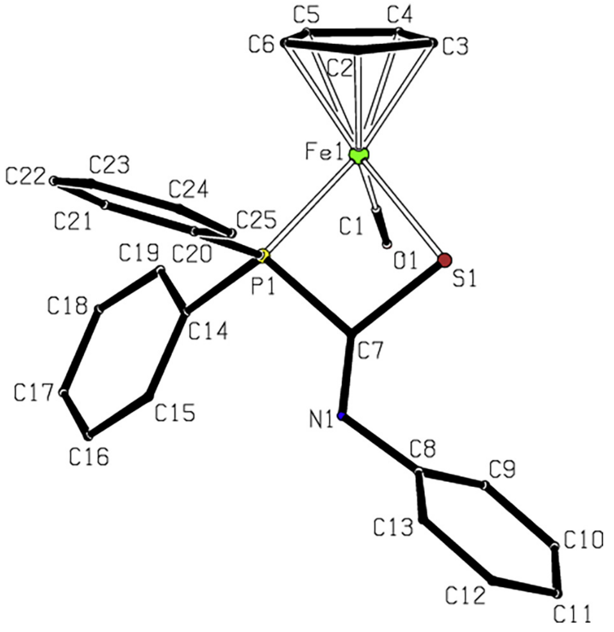

Fig. 2. PLATON view of **1**.

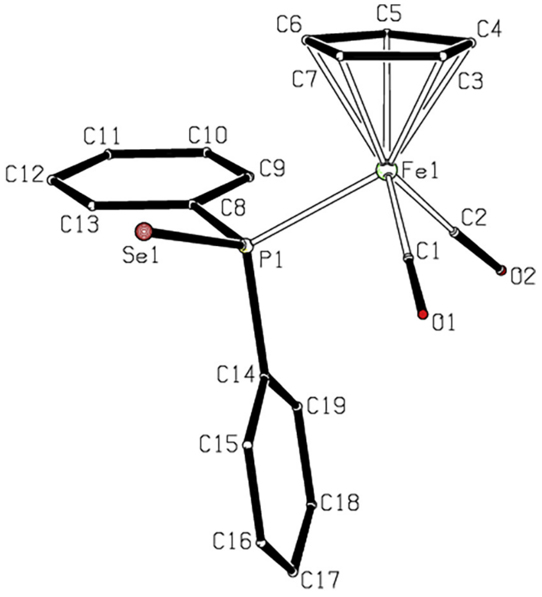

Fig. 3. PLATON view of **2**.

methods. Crystal data, selected bond lengths and angles (Å, °) are listed in Tables 1–2. Complex **1** adopts the geometry of a three-legged piano-stool, with Cp as the base and the one carbonyl and the $Ph_2PC(S){=}NPh$ ligand as the legs. The cyclopentadienyl ring (Cp) ligand is bonded to the Fe atom in an η^5-fashion with Fe—C bond distances ranging from 2.036(4) to 2.079(3) Å. The Fe-carbonyl bond distance of 1.744(3) Å is shorter than those (1.768(4), 1.780(4) Å) of $CpFe(CO)_2SCO_2Et$ [19]. The deprotonated ligand as PS donors is coordinated to the Fe atom, with the C7–N1 bond distance being 1.264(3) Å. The four-membered ring Fe1P1S1C7 is puckered, with the distance of Fe1 to plane P1S1C7 being 0.4331 (3) Å. The Fe—P bond distance is 2.1770(7) Å. The Fe—S bond distance of 2.3124(8) Å is larger than that (2.2675(10) Å) of $CpFe(CO)_2SCO_2Et$ [19].

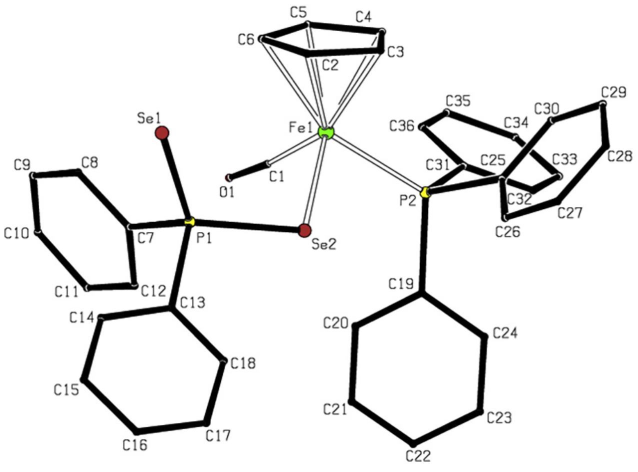

Fig. 4. PLATON view of **3**.

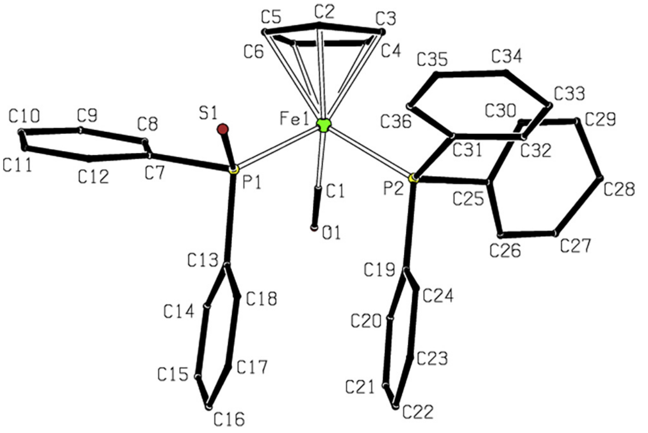

Fig. 5. PLATON view of **5**.

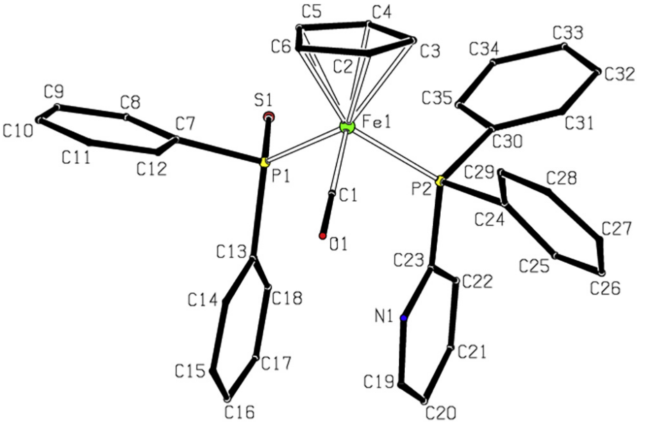

Fig. 6. PLATON view of **6**.

As shown in Figs. 3, 2 also contains the geometry of a three-legged piano-stool. The Cp ligand in an η^5-mode is coordinated to the Fe atom, with Fe—C bond distances ranging between 2.087 (4) and 2.107(5) Å. The Fe-carbonyl bond distances are 1.767(4) and 1.772(4) Å. The $SePPh_2$ ligand as a monoanion is linked to the Fe atom. The Fe—P bond length is 2.2577(10) Å with the P—Se bond distance of 2.1436(9) Å, indicating that the bond is a single bond [20].

Table 1
Crystal data, data collections and structure refinements for $Ph_2P(Se)CSNHPh$, **1**–**3** and **5**–**6**.

	$Ph_2P(Se)CSNHPh$	**1**	**2**	**3**	**5**	**6**
Formula	$C_{19}H_{16}NPSSe$	$C_{25}H_{20}FeNOPS$	$C_{19}H_{15}FeO_2PSe$	$C_{36}H_{30}FeOP_2Se_2$	$C_{36}H_{27}FeOP_2S$	$C_{35}H_{29}FeNOP_2S$
Fw	400.32	469.30	441.09	754.31	625.43	629.44
Crystal system	Orthorhombic	Monoclinic	Monoclinic	Monoclinic	Monoclinic	Monoclinic
Space group	*Pbca*	$P2_1/c$	$P2_1/n$	$P2_1/c$	$P2_1/c$	$P2_1$
a (Å)	11.9718(5)	15.0798(10)	11.0062(6)	18.4204(15)	10.7723(4)	11.2159(4)
b (Å)	8.7806(4)	10.2845(6)	12.1643(5)	11.571(1)	11.9828(6)	30.0279(11)
c (Å)	34.2265(16)	14.7903(10)	13.5707(6)	18.1814(15)	22.9556(11)	11.8440(5)
α (°)	90.00	90.00	90.00	90.00	90.00	90.00
β (°)	90.00	105.955(2)	93.470(2)	117.515(2)	93.102(1)	116.480(1)
γ (°)	90.00	90.00	90.00	90.00	90.00	90.00
V (Å^3)	3597.9(3)	2205.4(2)	1813.55(15)	3436.9(5)	2958.8(2)	3570.5(2)
Z	8	4	4	4	4	4
D_c (gcm^{-3})	1.478	1.413	1.615	1.458	1.404	1.171
μ (mm^{-1})	2.290	0.868	2.934	2.676	0.717	0.595
$F(000)$	1616	968	880	1512	1292	1304
Index ranges	$-15 \le h \le 15$	$-18 \le h \le 19$	$-14 \le h \le 12$	$-23 \le h \le 23$	$-13 \le h \le 13$	$-12 \le h \le 14$
	$-11 \le k \le 10$	$-13 \le k \le 13$	$-15 \le k \le 14$	$-14 \le k \le 15$	$-15 \le k \le 13$	$-38 \le k \le 37$
	$-44 \le l \le 44$	$-19 \le l \le 16$	$-14 \le l \le 17$	$-23 \le l \le 23$	$-26 \le l \le 29$	$-15 \le l \le 12$
Reflections measured	52533	22139	13379	30796	30530	40426
Unique reflections	4144	5069	4143	7858	6783	15054
Reflections ($I > 2\sigma(I)$)	3494	3679	3244	4948	4484	12721
R_{int}	0.037	0.037	0.043	0.072	0.050	0.028
θ Range (°)	2.9–27.6	2.4–27.6	2.5–27.6	2.2–27.6	2.5–27.5	1.4–27.5
Data/restraints/parameters	4144/0/212	5069/0/271	4143/0/217	7858/0/379	6783/0/389	15054/200/770
R_1	0.0360	0.0448	0.0488	0.0566	0.0508	0.0543
wR_2	0.1093	0.1229	0.1384	0.1409	0.1481	0.1590
Goodness-of-fit (GOF) on F^2	1.00	1.03	1.04	1.00	0.98	1.03
Largest difference in peak and hole (e Å^{-3})	0.66/−0.74	0.47/−0.30	0.54/−1.36	1.06/−0.97	0.73/−0.35	0.71/−0.48

Table 2
Selected bond lengths and angles (Å, °) for $Ph_2P(Se)CSNHPh$, **1**–**3** and **5**–**6**.

$Ph_2P(Se)CSNHPh$		**1**		**2**		**3**		**5**		**6**	
C1–N1	1.415(3)	Fe1–P1	2.1770(7)	Fe1–P1	2.2577(10)	Fe1–P2	2.2224(11)	Fe1–P1	2.2720(8)	Fe1–P1	2.2660(17)
C7–N1	1.320(3)	Fe1–S1	2.3124(8)	Fe1–C1	1.767(4)	Fe1–Se2	2.4267(7)	Fe1–P2	2.2349(9)	Fe1–P2	2.2168(16)
C7–S1	1.641(2)	C7–N1	1.264(3)	Fe1–C3	2.107(5)	Fe1–C1	1.751(5)	Fe1–C1	1.752(3)	Fe1–C1	1.721(7)
C7–P1	1.878(2)	C7–S1	1.759(2)	C8–P1	1.841(3)	Fe1–C2	2.121(4)	Fe1–C2	2.110(3)	Fe1–C2	2.119(7)
P1–Se1	2.1077(6)	C7–P1	1.832(2)	P1–Se1	2.1436(9)	P1–Se1	2.1194(12)	P1–S1	2.0044(11)	P1–S1	2.009(2)
		C8–N1	1.421(3)			P1–Se2	2.2003(12)			N1–C19	1.365(8)
						C1–Fe1–P2	96.06(15)				
N1–C7–S1	129.67(18)	S1–C7–P1	98.62(12)			C1–Fe1–Se2	97.32(15)	C1–Fe1–P2	91.63(10)	C1–Fe1–P2	91.3(2)
N1–C7–P1	111.40(17)	P1–Fe1–S1	74.63(2)	C8–P1–Se1	110.64(13)	P2–Fe1–Se2	88.17(3)	C1–Fe1–P1	93.67(10)	C1–Fe1–P1	94.5(2)
S1–C7–P1	118.90(14)	C7–P1–Fe1	93.73(8)	C8–P1–Fe1	112.19(12)	Se1–P1–Se2	118.15(5)	P2–Fe1–P1	101.19(3)	P2-Fe1–P1	100.34(6)
C7–P1–Se1	110.28(8)	C7–S1–Fe1	91.24(8)	Se1–P1–Fe1	111.56(4)	P1–Se2–Fe1	108.21(4)	S1–P1–Fe1	114.58(4)	S1–P1–Fe1	115.31(8)

Besides Cp, CO and PPh_3, **3** (Fig. 4) has a particular ligand $Ph_2PSe_2^-$. Fe–Cp bond distances are in the range of 2.074(4)–2.121(4) Å. The Fe-carbonyl bond distance of 1.751(5) Å is slightly shorter than that of **2**. The Fe–PPh_3 bond distance of 2.2224(11) Å is close to those found in the related iron complexes [2.230(1) Å; 17b]. The P—Se bond distances are 2.1194(12) Å for P1=Se1 and 2.2003(12) Å for P1-Se2. The Fe—Se bond distance is 2.4267(7) Å, which is slightly larger than that (2.3829(8) Å) of $CpFe(CO)_2SeCO_2Et$ [21]. Notably, the carbonyl is significantly bent, with the O1C1Fe1 bond angle being 172.6(4)°.

Complexes **5** and **6** are the corresponding monophosphine-substituted derivatives of $CpFe(CO)_2[kP\text{-}P(=S)Ph_2]$. As shown in Figs. 5 and 6, **5** and **6** also show the geometry of a three-legged piano-stool, with Cp as the base and CO, $SPPh_2$ and PPh_2R ligands as the legs. Unlike **5**, **6** has two different molecules in a unit cell. The Cp ligand is bound to the Fe atom with Fe—C bond distances of 2.097(3)–2.115(3) Å for **5** and 2.073(8)–2.119(7) Å for **6**. The Fe-carbonyl bond of 1.752(3) Å for **5** and 1.721(7), 1.747(6) Å for **6** is slightly shorter than those of $CpFe(CO)_2[kP\text{-}P(=S)Ph_2]$. The OCFe bond angle is 176.6(3)° for **5** and 175.6(6), 174.4(6)° for **6**. The Fe—P bond lengths are 2.2720(8), 2.2349(9) Å for **5** and 2.2660(17), 2.2168(16) and 2.2691(16), 2.2121(16) Å for **6**. The P—S bond distance is 2.0044(11) Å for **5** and **6** and 2.009(2), 2.009(2) Å for **6**. The FePS bond angle is 114.58(4)° for **5** and 115.31(8), 115.28(8)° for **6**. As a comparison, the corresponding values of $CpFe(CO)_2[kP\text{-}P(=S)Ph_2]$ (CCDC: YUCLOX) are listed as follows: Fe—C, 1.770, 1.773; Fe—P, 2.2605(6); P=S, 1.9906(7) Å; OCFe, 177.74, 178.47; FePS, 111.97° [12].

3.3. Spectroscopies

The synthesized complexes have been further characterized by IR, ^{1}H NMR, ^{13}C NMR and ^{31}P NMR (see Supplementary data, Figs. S1–S28). In the IR spectra, the terminal carbonyl group shows one strong absorption at 1944, 1933, 1935, 1929 and 1935 cm^{-1} for **1** and **3**–**6** except that **2** exhibits two absorptions at 2026 and 1974 cm^{-1}. In the ^{1}H NMR spectra of **1**–**6**, the phenyl and pyridyl groups are multiplets ranging from 8.72 to 6.76 ppm, the Cp group shows one singlet at 4.50, 4.93, 4.44, 4.52, 4.50 and 4.50 for **1**–**6**, respectively. In the ^{13}C NMR spectra, the terminal carbonyls as a doublet occur at 212.41, 212.18 ppm for **2** whereas those of **1** and **3**–**6** appear as a doublet or multiplet in the downfield range of 220.93–218.37 ppm. The Cp group displays one singlet at 81.09, 89.20, 89.14, 88.92, 81.14 and 81.12 for **1**–**6**, respectively.

The C═N group as one singlet occurs at 148.12 for **1**, but one multiplet at 158.71–147.61 ppm for **4** and two doublets at 150.28, 148.00 ppm (d, d, *J* = 13.0 Hz, *J* = 22.0 Hz) for **6**. The ^{31}P NMR spectra exhibit one singlet at 49.249, 75.889 ppm for **1**–**2** but two singlets at 76.61/53.06, 75.98/52.99, 76.12/73.95 and 76.14/74.30 ppm for **3**–**6**.

3.4. Electrochemistry

Cyclic voltammetry of **1**–**6** has been investigated to evaluate the capability of the new CpFe complexes to catalyze dihydrogen production (Figs. 7–12). According to the results proposed by Dempsey et al. [22], the average acid reduction potential versus Fc^+/Fc in 0.1 M $[Bu_4N][PF_6]$ of CH_3CN on GC is −2.36 ± 0.05 V for HOAc and −1.81 ± 0.03 V for TFA, therefore, as shown in Table 3, cyclic voltammetry of **1**–**6** in the presence of acids rules out direct reductions for acids. Except for **5**, all the other complexes in the absence of acids each show one irreversible oxidation and two irreversible reductions. Using TFA as a proton source, the second reduction peak of **1** exhibits catalytic behavior, the reduction current increases with increasing concentration of TFA added [23]. In the

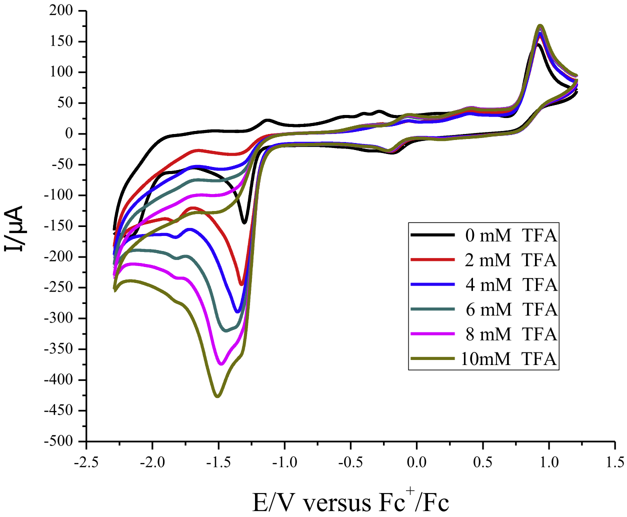

Fig. 9. Cyclic voltammograms of **3** (1.0 mM) with TFA (0–12 mM) in 0.1 M $^{n}Bu_4NPF_6$/MeCN at a scan rate of 100 mV s^{-1}.

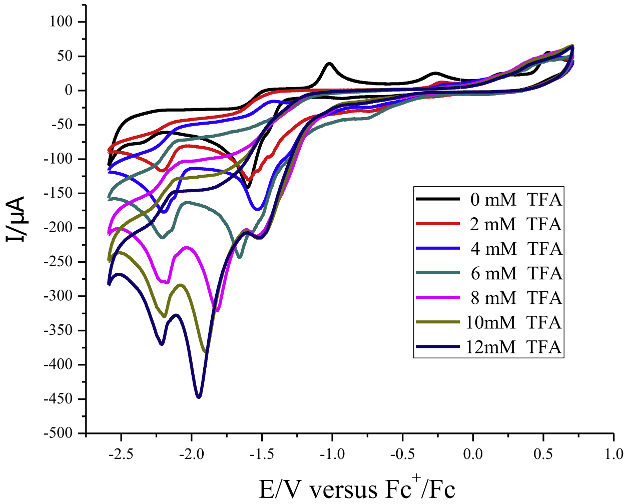

Fig. 7. Cyclic voltammograms of **1** (1.0 mM) with TFA (0–12 mM) in 0.1 M $^{n}Bu_4NPF_6$/MeCN at a scan rate of 100 mV s^{-1}.

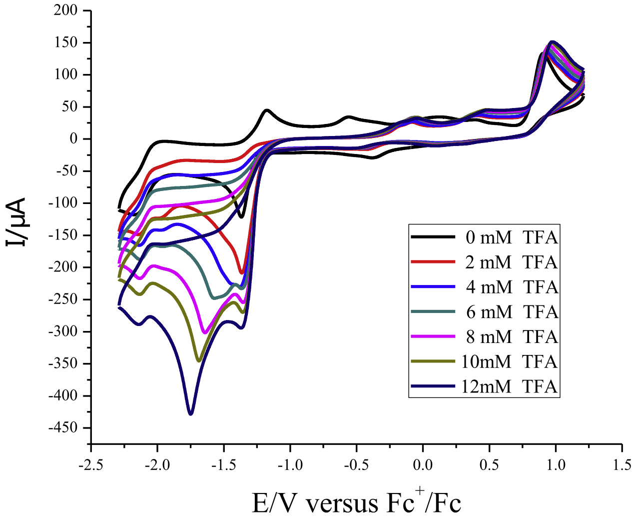

Fig. 10. Cyclic voltammograms of **4** (1.0 mM) with TFA (0–12 mM) in 0.1 M $^{n}Bu_4NPF_6$/MeCN at a scan rate of 100 mV s^{-1}.

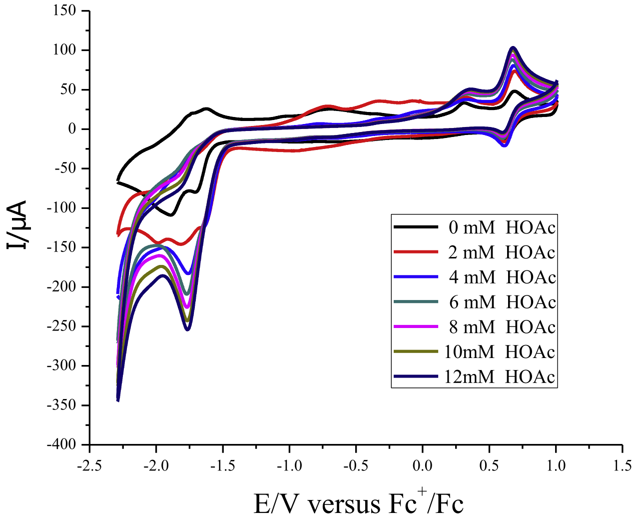

Fig. 8. Cyclic voltammograms of **2** (1.0 mM) with HOAc (0–12 mM) in 0.1 M $^{n}Bu_4NPF_6$/MeCN at a scan rate of 100 mV s^{-1}.

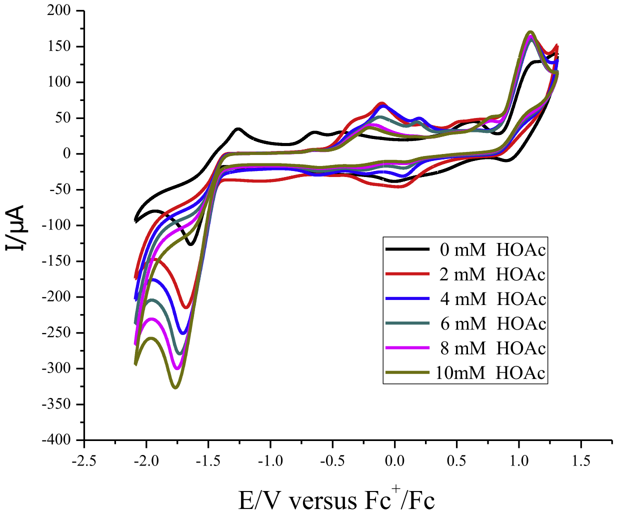

Fig. 11. Cyclic voltammograms of **5** (1.0 mM) with HOAc (0–12 mM) in 0.1 M $^{n}Bu_4NPF_6$/MeCN at a scan rate of 100 mV s^{-1}.

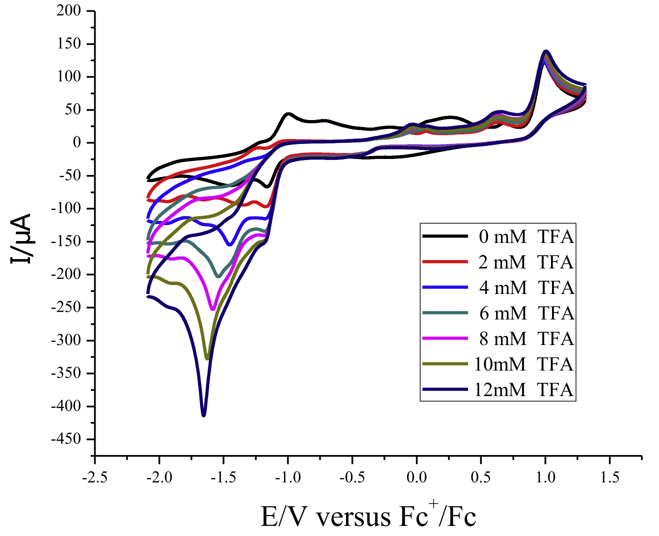

Fig. 12. Cyclic voltammograms of **6** (1.0 mM) with TFA (0–12 mM) in 0.1 M ^{n}Bu$_4$NPF$_6$/MeCN at a scan rate of 100 mV s^{-1}.

Table 3
Electrochemical data of **1–6** (0.1 M ^{n}Bu$_4$NPF$_6$/MeCN; scan rate, 100 mV s^{-1}; E vs Fc$^+$/Fc).

	E_{pc1}/V	E_{pc2}/V	E_{pa}/V
1	−1.60	−2.36	+0.53
2	−1.70	−1.89	+0.69
3	−1.30	−2.17	+0.92
4	−1.37	−2.17	+0.90
5	−1.65	–	+1.12
6	−1.16	−1.46	+1.00

presence of acetic acid, **2** with the second reduction can catalyze H_2 evolution. However, using TFA as a proton source, the first reductions of the other complexes display catalytic behavior. This fact supports that the pendent base can lower reduction potentials [4a,24]. The electrocatalytic activity of the CpFe complexes has been further confirmed by bulk electrolysis (Figs. 13–16). When bulk electrolysis of a MeCN solution of **1** (0.5 mM) with excess TFA (25 mM) or **2** (0.5 mM) with excess HOAc (25 mM) has been carried out for 1 h, a total of 19.4 and 16.4 F mol^{-1} passed, 9.7 and 8.2 turnovers are obtained. Moreover, gas chromatographic analysis shows that the yield of H_2 is about 83.7% and 73.3%, respectively. According to the defination of catalytic efficiency proposed by Evans et al. [2d], CE = (i_{cat}/i_d)/(C_{HA}/C_{cat}) (i_{cat}, catalytic

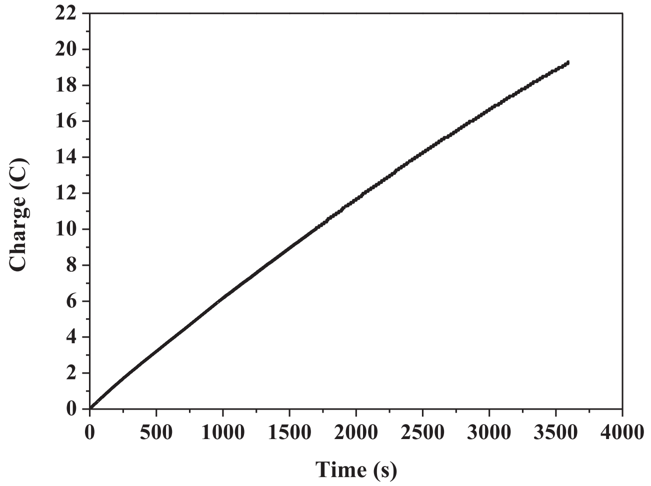

Fig. 13. Charge buildup vs time from electrolysis of **1** (0.5 mM) in 25 mM TFA.

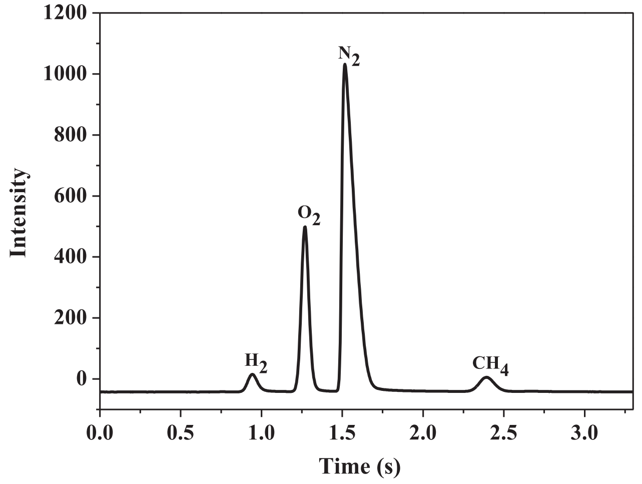

Fig. 14. GC traces after a 1 h controlled-potential electrolysis vs Ag/AgNO$_3$ of **1** (0.5 mM) in 25 mM TFA (CH_4 added for calibration purposes).

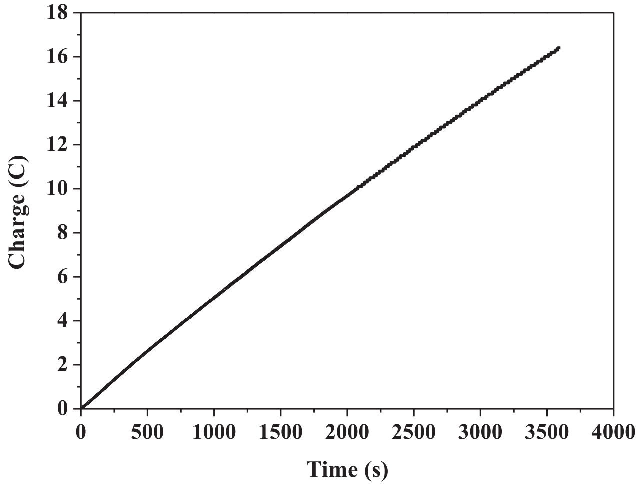

Fig. 15. Charge buildup vs time from electrolysis of **2** (0.5 mM) in 25 mM HOAc.

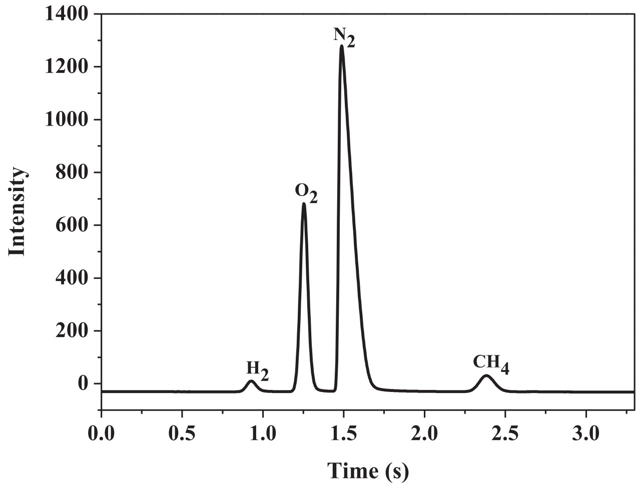

Fig. 16. GC traces after a 1 h controlled-potential electrolysis vs Ag/AgNO$_3$ of **2** (0.5 mM) in 25 mM HOAc (CH_4 added for calibration purposes).

current; i_d, current for reduction of the catalyst in the absence of acid; C_{HA}, acid concentration; C_{cat}, catalyst concentration), CE is calculated to be 0.71, 0.89 for **1**–**2**, 0.86, 0.91, 0.85, 0.81 for **3**–**6**, indicating that **1**–**6** are of high activity for H_2 production.

4. Conclusions

Six complexes of **1**–**6** have been synthesized by the reaction of $Ph_2P(Se)CSNHPh$ with $Cp_2Fe_2(CO)_4$ and the corresponding phosphine-substituted reaction of $CpFe(CO)_2(kP\text{-}P(=E)Ph_2)$ (E = S, Se) in the presence of Me_3NO. Electrochemical studies (Cyclic voltammetry and Bulk electrolysis) confirm that these CpFe complexes show catalytic H_2-producing activity in the presence of HOAc or TFA.

Acknowledgments

We are grateful to the Mao Zedong Foundation of China, Project Funded by the Priority Academic Program Development of Jiangsu Higher Education Institutions (PAPD), Postgraduate Research & Practice Innovation Program of Jiangsu Province (No. KYLX15_1356), Natural Science Foundation of China (No. 21472161, No. 20572091) and Natural Science Foundation of Jiangsu Province (No. 05KJB150151) for financial support of this work.

Appendix A. Supplementary data

Supplementary data associated with this article can be found, in the online version, at https://doi.org/10.1016/j.poly.2018.06.009.

References

[1] (a) W. Lubitz, H. Ogata, O. Rüdiger, E. Reijerse, Chem. Rev. 114 (2014) 4081;
(b) T.R. Simmons, G. Berggren, M. Bacchi, M. Fontecave, V. Artero, Coord. Chem. Rev. 270–271 (2014) 127;
(c) T. Xu, D.-F. Chen, X.-L. Hu, Coord. Chem. Rev. 303 (2015) 32;
(d) S. Dey, P.K. Das, A. Dey, Coord. Chem. Rev. 257 (2013) 42.

[2] (a) J.-F. Capon, F. Gloaguen, F.Y. Pétillon, P. Schollhammer, J. Talarmin, Coord. Chem. Rev. 253 (2009) 1476;
(b) C. Tard, C.J. Pickett, Chem. Rev. 109 (2009) 2245;
(c) D.M. Heinekey, J. Organomet. Chem. 694 (2009) 2671;
(d) G.A.N. Felton, C.A. Mebi, B.J. Petro, A.K. Vannucci, D.H. Evans, R.S. Glass, D.L. Lichtenberger, J. Organomet. Chem. 694 (2009) 2681;
(e) R. Mazzoni, A. Gabiccini, C. Cesari, V. Zanotti, I. Gualandi, D. Tonelli, Organometallics 34 (2015) 3228.

[3] (a) F. Gloaguen, T.B. Rauchfuss, Chem. Soc. Rev. 38 (2009) 100;
(b) W.-G. Wang, T.B. Rauchfuss, C.E. Moore, A.L. Rheingold, L.D. Gioia, G. Zampella, Chem. Eur. J. 19 (2013) 15476;
(c) T.B. Rauchfuss, Acc. Chem. Res. 48 (2015) 2107;
(d) D.L. DuBois, Inorg. Chem. 53 (2014) 3935;
(e) S. Raugei, D.L. DuBois, R. Rousseau, S.-T. Chen, M.-H. Ho, R.M. Bullock, M. Dupuis, Acc. Chem. Res. 48 (2015) 248;
(f) R.M. Bullock, M.L. Helm, Acc. Chem. Res. 48 (2015) 2017.

[4] (a) M.K. Harb, H. Görls, T. Sakamoto, G.A.N. Felton, D.H. Evans, R.S. Glass, D.L. Lichtenberger, M. El-khateeb, W. Weigand, Eur. J. Inorg. Chem. 2010 (2010) 3976;
(b) M.K. Harb, U.-P. Apfel, T. Sakamoto, M. El-khateeb, W. Weigand, Eur. J. Inorg. Chem. 2011 (2011) 986;
(c) R. Trautwein, L.R. Almazahreh, H. Görls, W. Weigand, Z. Anorg, Allg. Chem. 639 (2013) 1512.

[5] T. Xu, C.-J.M. Yin, M.D. Wodrich, S. Mazza, K.M. Schultz, R. Scopelliti, X.-L. Hu, J. Am. Chem. Soc. 138 (2016) 3270.

[6] P.J. Turrell, A.D. Hill, S.K. Ibrahim, J.A. Wright, C.J. Pickett, Dalton Trans. 42 (2013) 8140.

[7] D.-F. Chen, R. Scopelliti, X.-L. Hu, Angew. Chem. Int. Ed. 50 (2011) 5671.

[8] A.M. Royer, M. Salomone-Stagni, T.B. Rauchfuss, W. Meyer-Klaucke, J. Am. Chem. Soc. 132 (2010) 16997.

[9] (a) Y.-C. Shi, Y. Shi, J.-P. Li, Q. Tan, W. Yang, S. Xie, J. Coord. Chem. 68 (2015) 2620;
(b) Y.-C. Shi, S. Wang, S. Xie, J. Coord. Chem. 68 (2015) 3852.

[10] K. Issleib, G. Harzfeld, Chem. Ber. 97 (1964) 3430.

[11] G.S. Girolami, T.B. Rauchfuss, R.J. Angelici, Synthesis and Technique in Inorganic Chemistry, third ed., University Science Books, Sausalito, 1999, p. 177.

[12] I.-P. Lorenz, P. Murschel, W. Pohl, K. Polborn, Chem. Bev. 128 (1995) 413.

[13] (a) M.C. Burla, R. Caliandro, M. Camalli, B. Carrozzini, G.L. Cascarano, C. Giacovazzo, M. Mallamo, A. Mazzone, G. Polidori, R. Spagna, J. Appl. Crystallogr. 45 (2012) 357;
(b) G.M. Sheldrick, Acta Crystallogr. Sect. A. 64 (2008) 112.

[14] (a) A.L. Spek, Acta Crystallogr. Sect. D. 65 (2009) 148;
(b) L.J. Farrugia, J. Appl. Crystallogr. 45 (2012) 849.

[15] (a) M. El-khateeb, T. Obidate, Polyhedron 20 (2001) 2393;
(b) M. El-khateeb, Inorg. Chim. Acta 357 (2004) 4341;
(c) M. El-khateeb, Polyhedron 25 (2006) 1386;
(d) M. El-khateeb, H. Görls, W. Weigand, Inorg. Chim. Acta 360 (2007) 705;
(e) M. El-khateeb, A. Roller, Polyhedron 25 (2006) 1386.

[16] (a) M. El-khateeb, J. Mol. Struct. 1123 (2016) 300;
(b) M. El-khateeb, A. Mansor, I. Jibril, T. Rüffer, H. Lang, Polyhedron 133 (2017) 63.

[17] (a) A.A. Pasynskii, S.S. Shapovalov, Yu.V. Toruhaev, I.V. Skabitskii, O.A. Tikhonova, A.S. Sidorenkov, T.A. Krishtop, Russ. J. Coord. Chem. 40 (2014) 697;
(b) A.A. Pasynskii, S.S. Shapovalov, O.A. Tikhonova, I.V. Skabitskii, Yu.V. Toruhaev, S.G. Sakharov, Russ. J. Coord. Chem. 41 (2015) 741.

[18] J. Niemeyer, M.J. Kelly, I.M. Riddlestone, D. Vidovic, S. Aldridge, Dalton Trans. 44 (2015) 11294.

[19] M. El-khateeb, K.J. Asali, A. Lataifeh, Polyhedron 22 (2003) 3105.

[20] (a) Y.-C. Shi, Y. Shi, W. Yang, J. Organomet. Chem. 772–773 (2014) 131;
(b) J.-P. Li, Y.-C. Shi, J. Organomet. Chem. 866 (2018) 95;
(c) J.-P. Li, Y.-C. Shi, Inorg. Chim. Acta 482 (2018) 77;
(d) J.-P. Li, Y.-C. Shi, Polyhedron 151 (2018) 213.

[21] M. El-khateeb, Inorg. Chim. Acta 357 (2004) 4341.

[22] B.D. McCarthy, D.J. Martin, E.S. Rountree, A.C. Ullman, J.L. Dempsey, Inorg. Chem. 53 (2014) 8350.

[23] Y. Wang, M. Wang, L.-C. Sun, M.S.G. Ahlquist, Chem. Commun. 48 (2012) 4450.

[24] M. Wang, L. Chen, L.-C. Sun, Energy Environ. Sci. 5 (2012) 6763.